16

Recent Advances in Localization of Winding Deformation in a Transformer

Satish L
Indian Institute of Science
India

Ragavan K
Indian Institute of Technology Gandhinagar
India

1. Introduction

Power transformers are designed to withstand a variety of stresses and mechanical forces during their service life. Abnormal forces generated during short-circuits (occurring close to a transformer) is the main cause of deformation of winding and core. Rough transportation and unskilled handling is the other known cause. The cumulative effect of exposure to such abnormalities can lead to creation of a weak spot. Often, the damage leading to the creation of weak spot is not so severe to grossly impair its normal operation and hence immediately not perceivable. However, these weak spots provide favourable surroundings for the genesis of a fault, which grows and eventually leads to a catastrophic failure. In the present day scenario of deregulation and privatization, any unplanned outage is highly undesirable, and it is needless to elaborate its consequences. Therefore, a highly reliable and early detection of a winding deformation is paramount to enable timely initiation of preventive measures. Transformers are very bulky, so it is desirable to perform such status checks on-site and non-intrusively.

The normal operation of a transformer is the result of a synergic operation of several subsystems, such as, electrical, mechanical, thermal, insulation, etc. Over the years, monitoring and diagnostic tools have evolved to ascertain the status of these subsystems. So far as mechanical integrity of transformer windings and core is concerned, methods based on frequency response measurements, such as sweep frequency and transfer function, have a distinct advantage over the rest. Simply because, not only are the frequency-based methods highly sensitive in detecting even the slightest change in winding geometry (which constitutes a deformation), but can also be employed to estimate its location (as revealed by recent findings). This localization feature, although still in its infancy, makes this tool unique and worthy of further scrutiny. Driven by this motivation, recent progress by authors in localization of transformer winding deformation, using frequency-based technique, is presented.

2. Objective and Background

The frequency response of a transformer is highly sensitive to its winding geometry, distribution of winding capacitances and inductances, ground clearances, type of winding, and so on. Any physical change to the winding (either due to a deformation and/or a displacement) results in a change in some or all of these quantities, which in turn manifests as a change in the frequency response. More specifically, the peaks and troughs in the amplitude frequency response will exhibit a left or right shift. On some occasions, an additional peak may emerge or an existing one may disappear. Detection of any such deviation in frequency response, compared to the healthy frequency response (recorded earlier on the same transformer) implies that a winding damage might have occurred. Once such a condition is detected, the natural questions that arise are, (i) where along the winding is this damage located?, (ii) what is the extent of the damage and its seriousness? For answering these questions, obviously a non-invasive approach would be most attractive, as it would circumvent disassembly of the winding. Disassembling a winding is an expensive and time-consuming exercise, and this should evidently be the last resort. Therefore, the main objective is to demonstrate localization of winding deformation based on frequency response measurements.
A critical analysis of research performed so far, pertaining to this topic, reveals that all earlier efforts can essentially be grouped into the following categories, viz., detecting deformation in transformer windings (Lech & Tyminski, 1966; Dick & Erven, 1978; Rahimpour et al., 2003), assessing sensitivity and correlation between type of fault and measured quantity (Ryder, 2003; Florkowski & Furgal, 2003; Islam, 2000), and, developing circuit models and rational function approximations (Morched et al., 1993; Oguz Soysal, 1993; Gustavsen & Semlyen, 1999). As a matter of fact, there has been no previous attempt to localize deformation along a transformer winding using frequency response data, and hence it is worthy of consideration.

3. Approach

To achieve the goal of localization, it was considered worthwhile to construct a ladder network for representing the winding terminal behaviour, using the measured data. The reason for choosing a ladder network representation for this task is twofold-

1. The mutually coupled, lumped-parameter, ladder network is known to be best suited to represent all the intricacies of impulse behaviour of a transformer winding, and
2. It inherently captures the physical length of the winding, i.e. the physically continuous winding can be visualized as being mapped onto sections of the circuit, starting from line-end to the neutral-end.

In summary, the task essentially turns out to be a circuit synthesis exercise, subject to the constraint that the synthesized circuit must exhibit the same terminal characteristics as that measured. It is possible to synthesize an unique circuit by invoking the properties uniquely exhibited by driving-point functions and assuming a fixed circuit topology.
The approach essentially comprises of measuring the driving point impedance. From the amplitude frequency response plot of driving-point impedance, the frequencies corresponding to the peaks and troughs are identified and are referred to as open-circuit natural frequencies (ocnf) and short-circuit natural frequencies (scnf) respectively. For more details on extracting the ocnf and scnf values from the FRA plot, overcoming noise problems, etc, refer publication (Ragavan & Satish, 2007). This is nowadays a normal activity carried out by utilities and there exist commercial equipment to make these measurements. In addition to this, the effective

resistance, shunt capacitance and inductance are measured. Utilizing these measured data and some design information, the proposed method synthesizes a mutually-coupled, lumped parameter ladder network corresponding to each set of measurement. A comparison of these circuits with the reference reveals the location, as well as, the nature of damage.
When synthesizing a circuit, convergence is deemed to have occurred, when the differences between estimated and measured values of ocnf, scnf, effective capacitance and inductances are simultaneously less than a preset tolerance. Corresponding to every quantity, the error is calculated as-

$$\text{Percentage of Error} = 100 \times \frac{\text{Measured value - Estimated value}}{\text{Measured value}} \tag{1}$$

In addition to satisfying the tolerance, a manual inspection of the amplitude frequency response corresponding to the synthesized circuit and that measured is performed to ensure a one-to-one match throughout the frequency range of interest. Quite clearly, deformation localization in an actual multi-winding transformer is a very complex task, and poses several insurmountable difficulties. Here, a simplified version of the problem is discussed and solutions presented in three parts, with increasing order of complexity.

1. Initially, a model coil is considered. In this arrangement, discrete changes are introduced to a few elements at physically different positions along the model. Ability to accurately localize these changes is demonstrated.
2. Encouraged by the success and potential of the method, the approach is extended to an actual, single, continuous-disc interleaved winding of a transformer. Here, an iterative circuit synthesis approach is developed and localization of discrete changes, based on terminal measurements, is demonstrated.
3. The above iterative circuit synthesis approach is a brute-force method and takes tens of hours to synthesize even a 5-section ladder network. Obviously, localization accuracy achieved with such a small network is grossly inadequate and synthesizing large networks with this approach is simply ruled out. So, an entirely new, highly time-efficient algorithm (based on constrained optimization techniques) capable of synthesising large-sized ladder networks (within tens of seconds) is presented. Thus, in principle, it paves way for extending this method to multiple windings, which is the ultimate goal.

4. Specimens and Measurement Setup

Experiments were conducted on three specimens, viz. a model coil, a continuous-disc interleaved winding, and a continuous disc winding. The model coil consisted of a single-layer winding wound on an insulating air-core former of diameter 200 mm. The winding had 200 turns and taps were provided after every 20 turns. Using these taps, series and shunt capacitances could be externally connected to represent either a continuous disc, interleaved or partially interleaved winding. At the taps, specific changes at any location along the model coil could be introduced. The model coil along with the FRA measurement setup is shown in Fig. 1.
The other two specimens are actual transformer windings, specifically built for this purpose. They are wound on an insulating air-core former, and each had 16 discs with 10 turns per disc. The copper turn had a cross-section of 18 sq mm and the insulation thickness, duct spacing, etc. corresponded to 11-kV rating. It had a total height of 215 mm, inner and outer diameter of

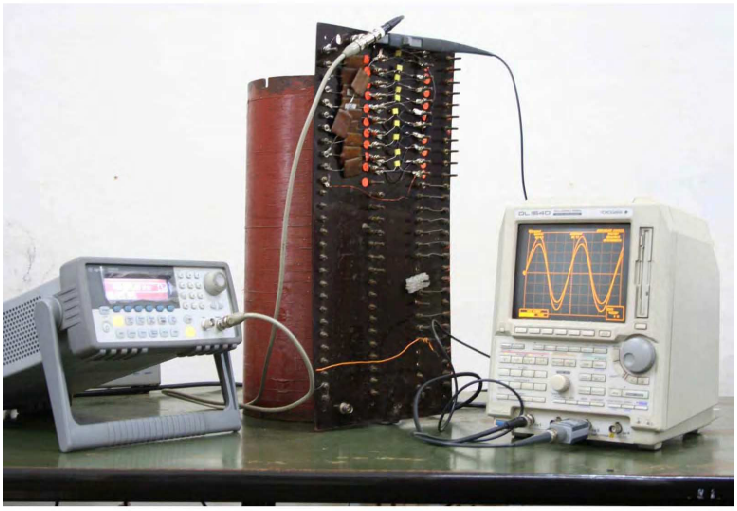

Fig. 1. Experimental arrangement for frequency response measurements on a model coil

260 and 350 mm respectively. Of the two actual windings, the first was fully interleaved, while the second was entirely of disc-type. These windings were placed on an aluminium sheet and another concentrically placed inside to represent the ground plane. Since, the magnetic flux at higher frequencies is predominantly confined to the outer surface of the core, it is justifiable to neglect the presence of the core in this work. In order to introduce discrete changes, the outer and top portions were kept uncovered. Experimental arrangement together with the interleaved winding is shown in Fig. 2.
The effective inductance and ground capacitance were measured by an LCR bridge at 1 kHz, while the dc resistance was measured by a multimeter. The driving point impedance was measured automatically (refer to Satish & Santosh C Vora, 2009 for details) by sweep frequency measurements (and cross verified by the manual sweep method) using (i) an arbitrary waveform generator producing 20 Vp-p sinusoid with frequency range of 0-80 MHz, (ii) a 150 MSa/s, 8-bit digital oscilloscope and (iii) a clamp-on current probe with sensitivity of 2 mA/mV and bandwidth of 450 Hz to 60 MHz. All signals were connected with a 50 Ω coaxial cable and the oscilloscope was terminated by 50 Ω. A sample of the amplitude frequency response for each specimen (reference case) is included while discussing the results.

5. Discrete Changes

Transformer winding deformation is classified into radial, axial, presence of eccentricity, loss of clamping pressure, and so on. The severity and extent of damage, among other factors, depends on the short circuit force magnitude. The damage suffered by the winding is, at times, confined to only a few discs or as most often observed, affects a majority of the discs in the entire winding. So far, in spite of several investigations, there seems to emerge no particular pattern that correlates the nature of winding damage to measurable quantities at

Fig. 2. Experimental arrangement for frequency response measurements on an interleaved winding

the terminals. Inability to generalize this wide variability makes any investigation, and in particular the task of localization, all the more complex. Nevertheless, to make a beginning in this regard, deformations considered in this work are discrete and confined to a small part of the winding. In other words, they are intended to be localized and specifically cause an increase or decrease of the capacitance or inductance in the winding. Since their location and extent is precisely known a priori, it assists in developing and fine-tuning the proposed methodology. Once an acceptable method to address this task emerges, further studies by incorporating actual deformations in windings can be undertaken.

Specifically, deformations in this work are represented by a discrete change of the following two types- (i) addition of some tens of pico-farads of capacitance at a particular disc to ground, resulting in a predominant increase in shunt capacitance, and/or (ii) short-circuiting of a few turns within a disc, introducing a predominantly inductive change. These changes introduced could be more than one in number and be physically occurring at different positions along the winding. Also, any combination of these changes could be introduced in the winding at a time. Thus, it will be interesting to investigate how simultaneous changes can be correctly localized. Also, there may or may not be any net change in the effective capacitance, after these changes are made. After discrete changes are incorporated, a new set of ocnf and scnf are measured along with other parameters. Lastly, the deformations considered in this work are not like the real ones (radial, axial etc.) arising in practice. Despite this, the effort is still considered noteworthy, since deformation localization based on terminal measurements on a transformer winding has, so far, not been attempted.

6. Experimental Results on a Model Coil

6.1 Underlying Principle

The first step in the proposed method involves representing the model coil by means of a ladder network, called the reference circuit. To achieve this, the following quantities of the model coil, resistance, R; equivalent air-core inductance, L_{eq}; effective shunt capacitance to ground, $C_{g,eff}$; and initial voltage distribution constant α are required. Among these, except α, all the remaining quantities are measurable at the input terminals of the model. The initial voltage distribution constant, α, can be got from design details. The steps involved in synthesizing a circuit to represent the model coil are as follows.

- Determine natural frequencies (ocnfs and scnfs) of the model coil by sweep frequency measurements.
- Determine the number of sections (N) of the ladder network to be synthesized.
- Estimate individual values of the elements of the ladder network. Let K_{ref} and L_{ref} be the nodal capacitance and inductance matrices respectively corresponding to the reference circuit.

Details of these steps along with the pseudo code for the algorithm are described in (Ragavan & Satish, 2007). For brevity these details have been omitted. Synthesis of the circuit after introduction of changes essentially consists of the following steps-

- The measurements are repeated after a few elements in the model coil are changed. From the frequency response, ocnfs and scnfs are identified. A comparison of these frequencies with those corresponding to the reference case is made. A deviation greater than 2% would indicate that a new circuit has to be synthesized.
- Using the new set of measured values another ladder network is synthesized. For this purpose, the matrices describing the reference circuit are used as the initial guess. Its elements are iteratively varied until the estimated and measured effective inductance, effective shunt capacitance, and the natural frequencies are well within 2% tolerance.
- Let K_{est} and L_{est} be the capacitance and inductance matrices respectively corresponding to the model coil after changes. A comparison of those matrices with K_{ref} and L_{ref} reveals the elements that have changed. The row and column of the changed element in the matrix reveals the position along the model coil where the changes have been made. Further, the extent of change and whether the change is confined to inductances and/or capacitances can also be ascertained.

6.2 Reference Circuit

The measured magnitude and phase plots of the driving-point impedance corresponding to a continuous-disc model coil (reference or healthy case) are presented in Fig. 3. From the plot, the ocnf and scnf can be extracted and are presented in Table 1. Then the following quantities, viz. $R = 8\ \Omega$, $L_{eq} = 6.98$ mH and $C_{g,eff} = 5.6$ nF were measured on the model coil.
Employing the method described in (Ragavan & Satish, 2007), a ladder network having the same set of natural frequencies as measured with the model coil is synthesized. Details of how the number of sections of the ladder network was decided are described in (Ragavan & Satish, 2007). The self and mutual inductances are estimated iteratively and presented in Table 2. Corresponding to the model coil shown in Fig. 4(a), a 6-section ladder network was synthesized and is shown in Fig. 4(b). The estimated driving-point impedance corresponding

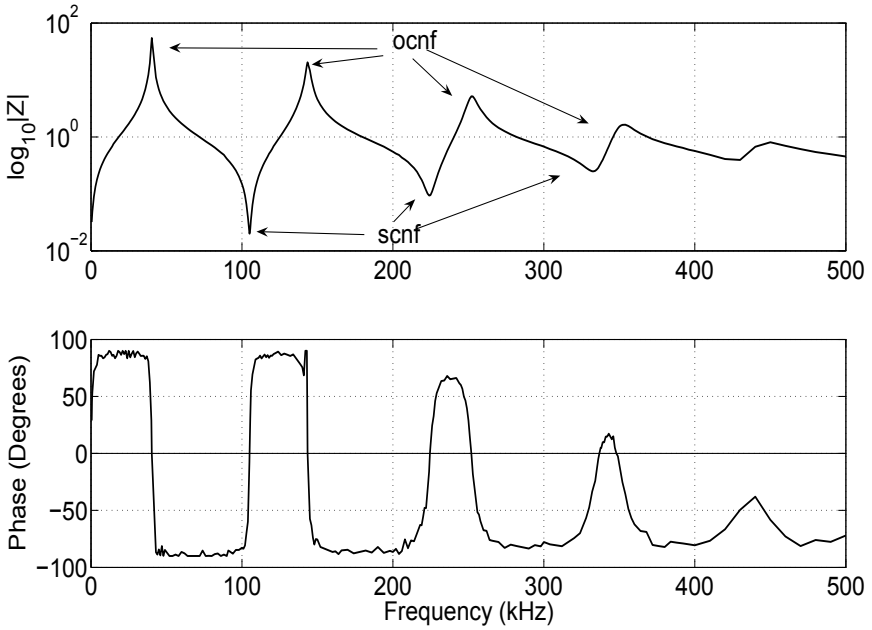

Fig. 3. Measured driving-point impedance for model coil (continuous disc representation) - Reference Case

ocnf	Measured	40.3	143	250.6	346
(kHz)	Estimated	40.48	142.58	249.42	346.41
scnf	Measured	105	223.8	336	-
(kHZ)	Estimated	105.19	224.79	334.44	-

Table 1. Measured and estimated natural frequencies for model coil (continuous disc representation) - Reference Case

L_s	$M_{i,i+1}$	$M_{i,i+2}$	$M_{i,i+3}$	$M_{i,i+4}$	$M_{i,i+5}$
0.4310	0.2392	0.1435	0.0947	0.0612	0.0496

Table 2. Estimated self and mutual inductances (in mH) for circuit in Fig. 4(b)

to the synthesized circuit is shown in Fig. 5. A comparison of the computed driving point impedance with the measured clearly shows the excellent match and accuracy achieved by the synthesized circuit. The next step is to introduce changes and repeat the exercise. The changes made in the model coil were confined only to capacitive changes, since, due to practical difficulties in the available model coil, desired inductive changes could not be made. However, case studies with inductive changes will be presented and discussed in Section 7.

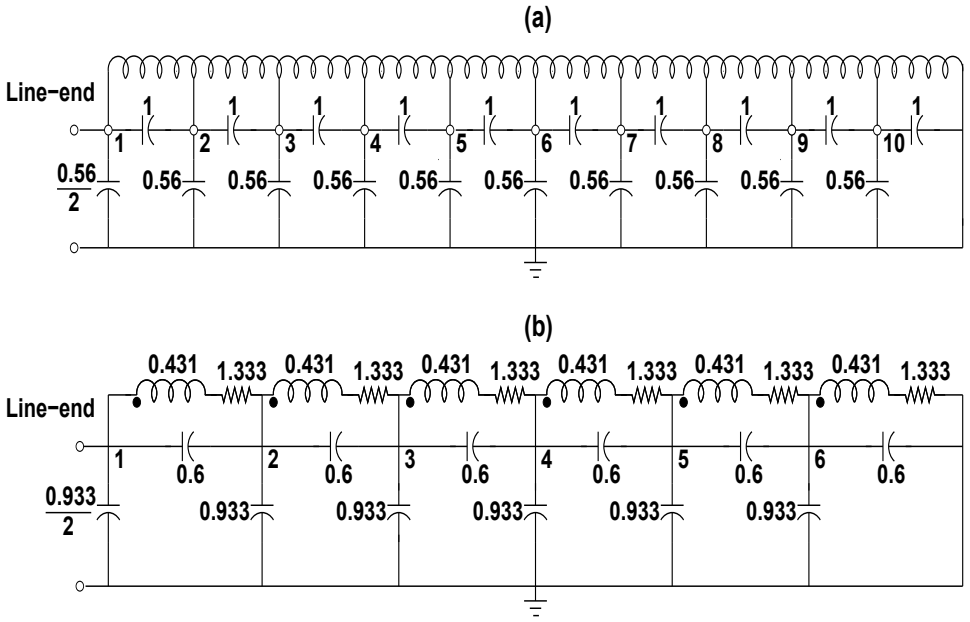

Fig. 4. Reference case (a) Model coil, (b) Synthesized circuit (Note: Elemental values are in Ω, nF, mH. Mutual inductances of synthesized circuit are given in Table 2)

6.3 Case-A, Capacitive Changes Occurring at Physically Connected Taps

In these experiments, capacitive changes are introduced at more than one tap in the model coil. For example, series capacitance between TAPS 3 and 4 was decreased from 1 to 0.56 nF, and shunt capacitance at TAP 4 was increased from 0.56 nF to 1 nF (Fig. 6(a)). Thus, there are two simultaneous changes occurring in the model coil which have to be localized. The new set of ocnf and scnf were measured and are indicated in Table 3. These changes introduced in the model coil manifest as a decrease and increase of the capacitances linked to the NODES 2 and 3 respectively, in the synthesized circuit shown in Fig. 6(b). Thus, it is evident that not only have all changes introduced been accurately localized, their nature has also been correctly identified. Some of the discrete changes introduced in the model coil were not correspondingly reflected by the same number of discrete changes in the synthesized circuit. This aspect should not be construed as an error. This arises because all taps in the model coil are not mapped on to discrete nodes in the synthesized circuit. This matter is explained while discussing mapping between model coil and synthesized circuit, in Section 6.6

6.4 Case-B, Capacitive Changes Occurring at Physically Separated Taps

In reality, mechanical deformations often result in damages that affect different parts of the winding. Hence, it is interesting to simulate such a situation to the extent possible. With this in mind, in this experiment, capacitances at TAPS 1 (line end) and 6 (middle) were simultaneously increased and decreased, respectively, by the same margin (Fig. 7(a)). As a result, the net change in effective capacitance was zero. The corresponding frequencies identified from

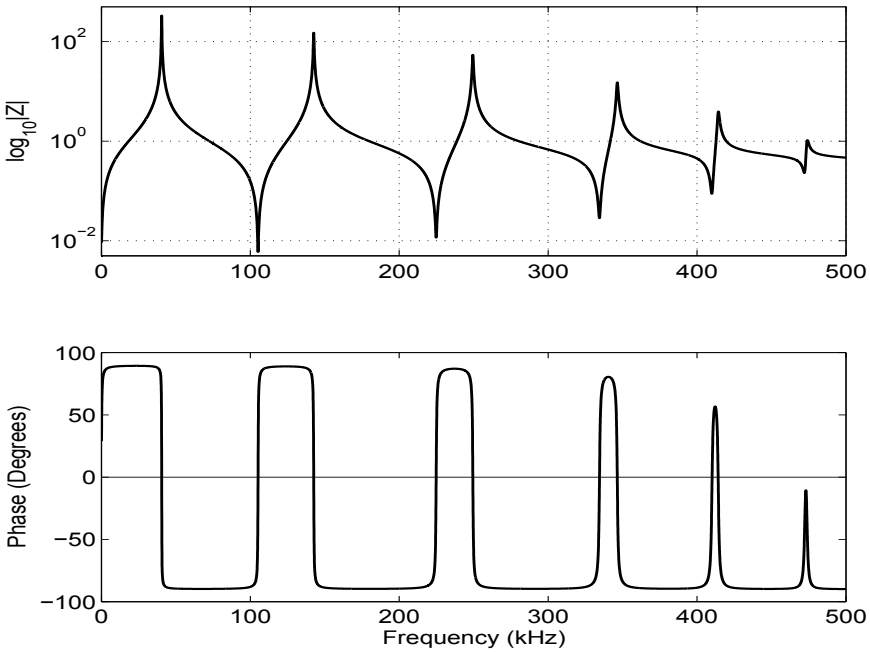

Fig. 5. Driving-point impedance estimated using synthesized circuit in Fig. 4(b)

ocnf	Measured	38.4	144.6	246.8	341
(kHz)	Estimated	39.15	143.68	244.74	346.82
scnf	Measured	101.3	216.7	331	-
(kHz)	Estimated	101.52	219.54	337.52	-

Table 3. Measured and estimated natural frequencies for model coil (continuous disc representation) - Fault Case A

FRA are mentioned in Table 4. The synthesized circuit for this case was obtained following

ocnf	Measured	38.8	141	245.3
(kHz)	Estimated	39.01	140.16	244.03
scnf	Measured	110	224.9	-
(kHz)	Estimated	109.51	224.81	-

Table 4. Measured and estimated natural frequencies for model coil (continuous disc representation) - Fault Case B

the same procedure and is shown in Fig. 7(b). From the results, it is found that the changes

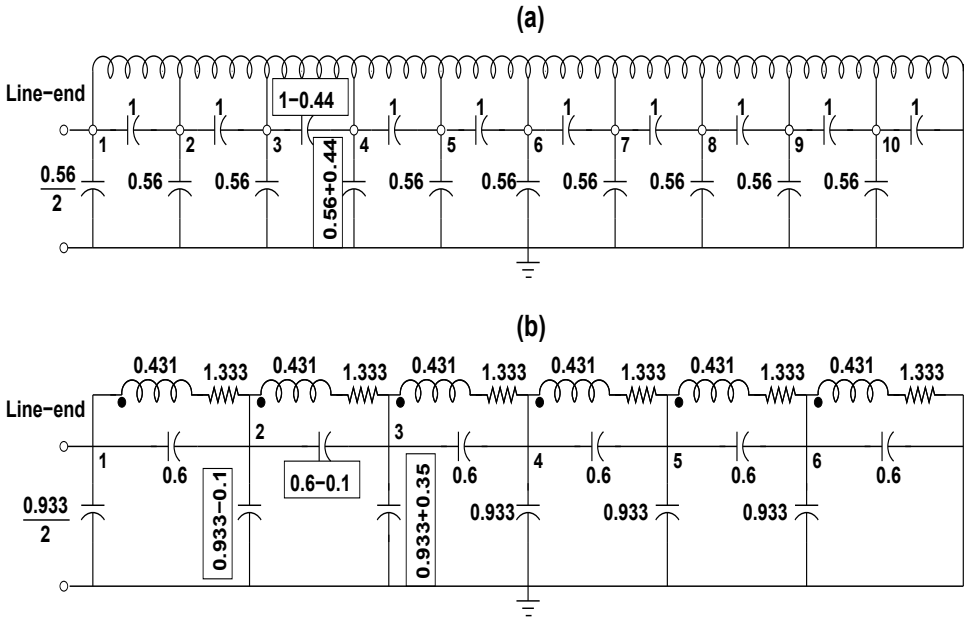

Fig. 6. Fault Case-A (a) Model coil, (b) Synthesized circuit (changes made and predicted are encircled)

were reflected at NODES 1 (line end) and 4 (middle) in the synthesized circuit. Despite no net change in the value of effective capacitance, the method was able to correctly identify the changes made in the model coil. This demonstrates the ability of the method to identify multiple changes occurring at physically different locations along the model coil.

6.5 Case-C, Experiments with Partially Interleaved Representation

The previous two case studies involved a uniform continuous disc representation. It would be interesting to examine the applicability of this method for a partially interleaved representation. In a partially interleaved winding, initial voltage distribution constant would be different for different parts of the winding. In this study, a partially interleaved representation (i.e. 20%) is considered as shown in Fig. 8(a), wherein the first two sections have double the series capacitance compared to the rest. Natural frequencies of this model coil are mea-

ocnf	Measured	40.7	151.2
(kHz)	Estimated	40.9	149.27
scnf	Measured	107.62	-
(kHz)	Estimated	107.86	-

Table 5. Measured and estimated natural frequencies for model coil (partially interleaved representation) - Reference Case

sured and presented in Table 5. Calculations showed that $N = 5$. Since the percentage of

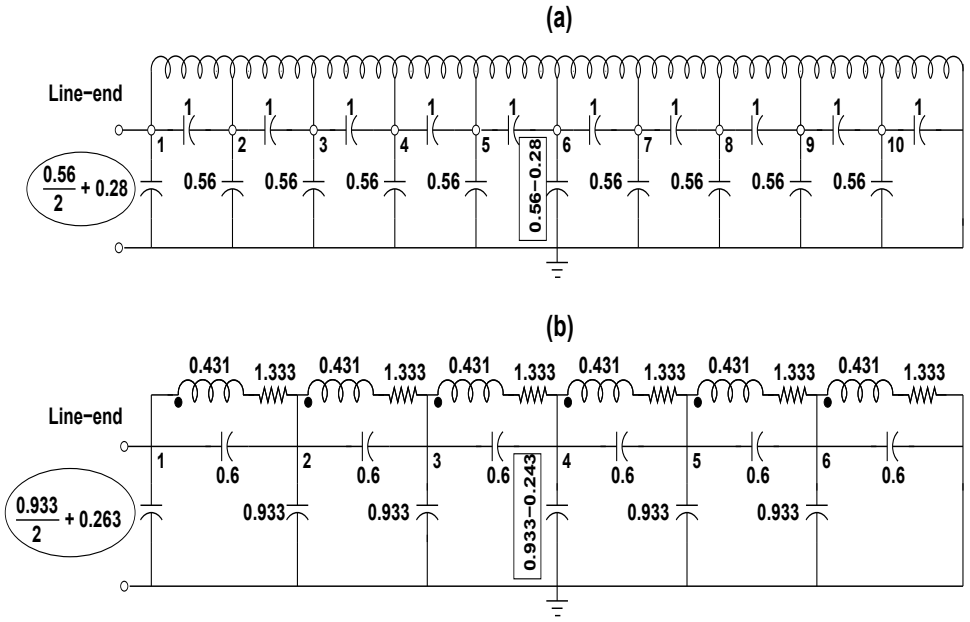

Fig. 7. Fault Case-B (a) Model coil, (b) Synthesized circuit (changes made and predicted are encircled)

interleaving is 20%, an attempt was made to synthesize a 5-section equivalent circuit in the ratio of 1:4 and is shown in Fig. 8(b).

With this model coil, case studies similar to those presented earlier were repeated. In all of them, it was observed that the changes estimated by the synthesized circuit corresponded to the changes introduced in the model coil. One sample result is presented here.

In Fig. 9(a), C_g at TAP 5 was decreased from 0.56 nF to 0.1 nF and C_s between TAPS 1 & 2 and 2 & 3 were increased from 1 nF to 2 nF. In Table 6, new set of measured natural frequencies for this case are given. The corresponding synthesized circuit is shown in Fig. 9(b). The net series capacitance change is only 0.5 nF, which is predicted as a 0.33 nF change in the synthesized circuit. The shunt capacitance change in the model coil is 0.46 nF and this is identified as a change of 0.4 nF in the synthesized circuit. Thus, the changes introduced in the model coil were correctly identified in the synthesized circuit shown in Fig. 9(b). The changed and predicted elements are encircled, in the figure. Thus, it has been shown that the method works equally well for both types of winding representations.

ocnf	Measured	42.7	146.6
(kHz)	Estimated	42.67	146.56
scnf	Measured	112.63	-
(kHz)	Estimated	112.71	-

Table 6. Measured and estimated natural frequencies for model coil (partially interleaved representation) - Fault Case C

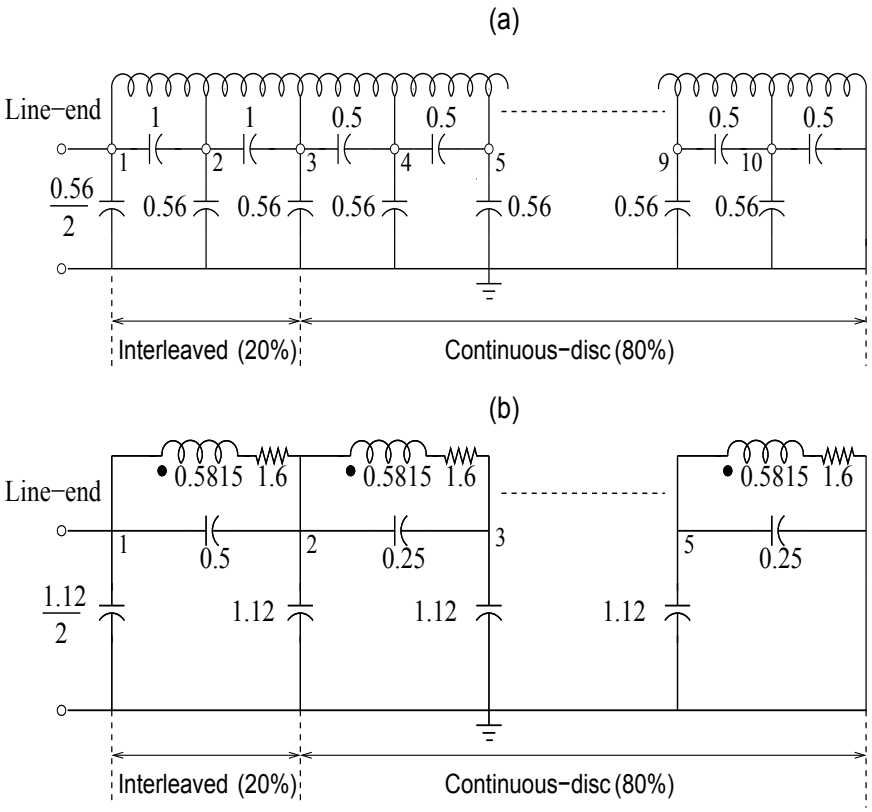

Fig. 8. Reference case (a) Model coil (partially interleaved), (b) Synthesized circuit

6.6 Mapping of Taps in Model Coil to Nodes in Synthesized Circuit

In the case studies corresponding to Fig. 6 and Fig. 7, the actual position of the changes introduced in the model coil were accurately localized, by observing the elements in the synthesized circuits that have changed. From these results, it emerges that a correlation exists between the model coil and the synthesized circuit. This is schematically shown in Fig. 10 along with the mapping results, which link changes introduced at taps in the model coil to the nodes in the synthesized circuit. The next step is to implement the proposed method on an actual transformer winding.

7. Experimental Results on an Actual Transformer Winding (Fully Interleaved)

When considering an actual winding, the following issues are to be addressed additionally as opposed to the model coil.

- In an actual winding, the capacitances (shunt and series) and inductance are all truly distributed, in contrast to discrete series and shunt capacitances used in a model coil and crucially depend on the physical disposition of discs/conductors, clearances to

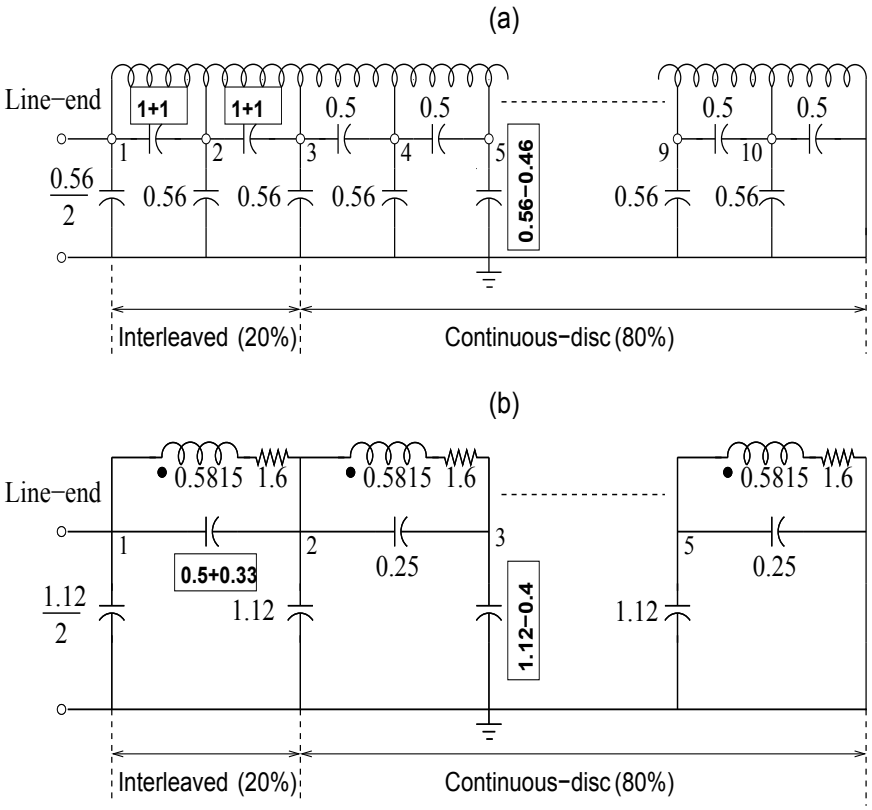

Fig. 9. Fault Case - C (a) Model coil (partially interleaved), (b) Synthesized circuit (changes made and predicted are encircled)

ground, thickness of insulation, etc. Hence, while estimating shunt capacitances, the condition of uniform distribution cannot be invoked here.

- The initial voltage distribution constant (α) in an actual winding, needs to be iteratively estimated, as opposed to a model coil (where series and shunt capacitances can be readily determined). For an interleaved winding (under consideration in the present case), lower and upper bounds for α can be chosen as two and four respectively.
- Capacitive changes (increase and/or decrease) in a model coil were manifested as capacitance changes at pertinent nodes (Ragavan & Satish, 2007). However, when inductance is changed (essentially short-circuiting a few turns), it does not manifest as a discrete change in the synthesized circuit, but affects the self and all mutual inductances (i.e. results in a widespread change to the entire inductance matrix). Therefore, suitable modifications have to be built into the circuit synthesis procedure to account for inductive and/or capacitive changes. Furthermore, due to loss of symmetry in the inductance matrix following an inductive change, each individual element of the in-

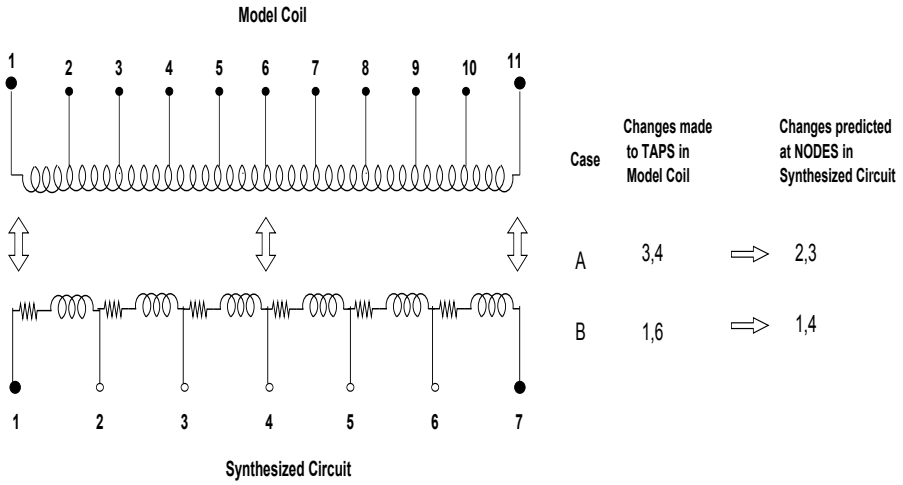

Fig. 10. Mapping of taps in model coil to nodes in synthesized circuit (series and shunt capacitances exist both in model coil and synthesized circuit, but those are not shown)

ductance matrix needs to be iteratively estimated, thereby significantly increasing the computational burden.

- Lastly, whenever an actual mechanical deformation occurs, in order to enable its correct representation, it is obvious that both inductive and capacitive changes have to be simultaneously considered. Keeping in mind this very essential requirement, while formulating a solution for an actual winding, simultaneous inductance and capacitance change feature was built in.
- Compared to the solution for model coil, the solution for an actual winding involves iterative estimation of several quantities, and each of them has to be chosen from a large search-space. To be precise, as opposed to estimating two parameters (viz. self and mutual inductances), a total of five parameters (viz. number of sections, initial voltage distribution constant, shunt capacitance, self and mutual inductances) have to be iteratively estimated in the present case. Thus, synthesizing a circuit for an actual winding is computationally intensive and requires a lot of computer time, even for a reasonably small-sized circuit to be synthesized.

For the above stated reasons, synthesizing a circuit for an actual transformer winding (from measured data) is a far more onerous task, compared to the model coil problem dealt in the previous section.

Lastly, introduction of mechanical deformation to the actual winding (done by other researchers such as Lech & Tyminski, 1966; Dick & Erven, 1978; Rahimpour et al., 2003; Ryder, 2003) was not possible in the present experimental setup. So, as a first approximation, only discrete changes (capacitive and/or inductive) were introduced at selected positions along the winding. Such a procedure achieves the desired goal of introducing a change in inductance and/or capacitance at specified positions on the winding. Furthermore, it assists in checking the correctness of the obtained results.

From measured values of ocnf, scnf, effective capacitance ($C_{g,eff}$), inductance (L_{eq}) and resistance (R), and a knowledge of the type of winding, a lumped-parameter ladder network is iteratively synthesized so as to closely match (within a specified tolerance) the measured driving-point impedance. The circuit thus obtained is called the reference circuit. After introducing a change, all the measurements are repeated. If any of the ocnf or scnf differs by more than 2% of the corresponding reference value, then a change is deemed to have occurred and a new circuit is synthesized. Details of the algorithm is described in (Satish & Subrat K Sahoo, 2009).

7.1 Reference Circuit

The interleaved winding in Fig. 2 is considered for this work. The driving-point impedance corresponding to the reference (or healthy) case was measured and is shown in Fig. 11[A]. From this, three ocnf peaks could be counted, and hence it was taken as the initial value for N. Since, it was an interleaved winding, the initial value of α was taken as 2, and allowed to vary up to 4, in small steps. The effective inductance, capacitance and resistance were measured and found to be 4.9 mH, 0.37 nF and 0.3 Ω respectively. Convergence is obtained when all the estimated and measured ocnf and scnf satisfy the 2% tolerance limit. The converged values of inductance and capacitance were 5 mH and 0.37 nF respectively. This is pictorially observable from the estimated impedance plot in Fig. 11[B]. The number of sections and the value of α were estimated as 5 and 2.8, respectively. Thus, out of a total of 16 discs, roughly 3 discs of the winding are mapped to each section of the synthesized circuit. The synthesized reference circuit is shown in Fig. 12, while the estimated self and mutual inductances are listed in Table 7.

L_s	$M_{i,i+1}$	$M_{i,i+2}$	$M_{i,i+3}$	$M_{i,i+4}$
0.440	0.220	0.090	0.085	0.080

Table 7. Estimated self and mutual inductances (in mH) for circuit in Fig. 12

7.2 Case-D, Inductive Change at Line-end

This example pertains to a condition wherein the inductance has changed predominantly. This is achieved by shorting the outermost turns of disc number 2 and 3. The effective inductance decreased by 200 μH while the effective capacitance remained unchanged. The driving-point impedance was measured and the identified ocnfs and scnfs are presented in Table 8. The

ocnf	Measured	201	399	523
(kHz)	Estimated	204.7	403.3	532.7
scnf	Measured	338	499	-
(kHz)	Estimated	334.8	507.9	-

Table 8. Measured and estimated natural frequencies for an actual transformer winding (interleaved) - Case D

deviation of natural frequencies is beyond 2% with respect to the reference and hence a new circuit (with topology fixed at 5 sections) needs to be synthesized. Following the procedure described, a new circuit was synthesized. The natural frequencies of the synthesized circuit

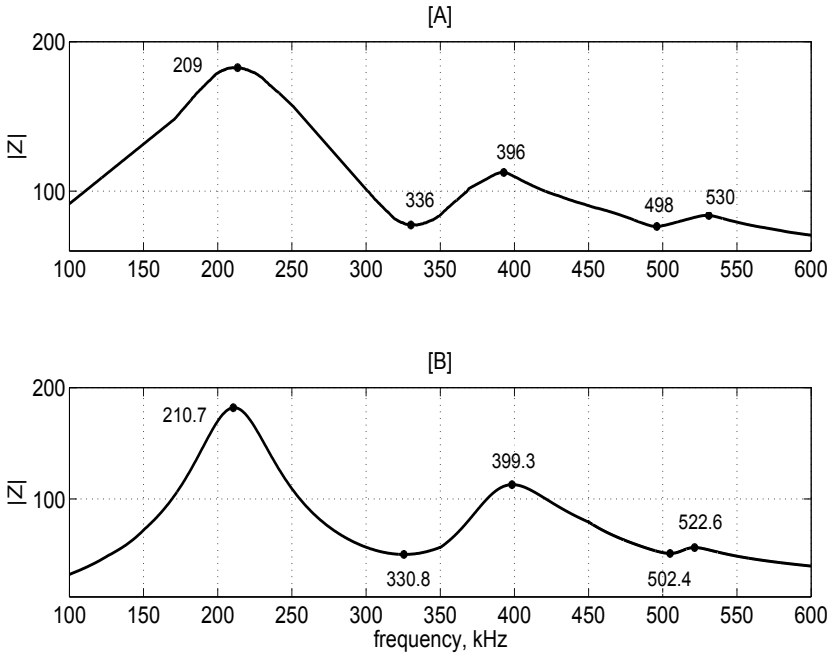

Fig. 11. Driving-point impedance for an actual transformer winding (Interleaved), Reference case, [A] Measured, [B] Estimated

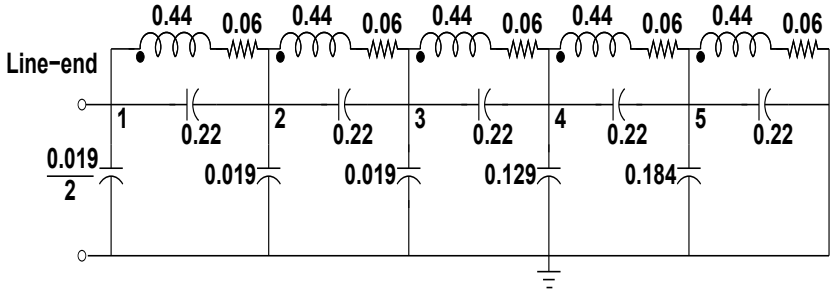

Fig. 12. Reference circuit pertaining to an actual transformer winding (interleaved) (Note: Elemental values are in Ω, nF, mH. Mutual inductances of synthesized circuit are given in Table 7)

are also presented in Table 8. The convergence criterion has been satisfied and the match between estimated and measured characteristics was observed to be good. The converged

values of inductance matrix is given below.

$$L_{est,D} = \begin{bmatrix} 0.400 & 0.190 & 0.080 & 0.075 & 0.070 \\ 0.190 & 0.430 & 0.210 & 0.090 & 0.085 \\ 0.080 & 0.210 & 0.435 & 0.215 & 0.090 \\ 0.075 & 0.090 & 0.215 & 0.435 & 0.220 \\ 0.070 & 0.085 & 0.090 & 0.220 & 0.440 \end{bmatrix} \quad (2)$$

Node	Line		$\Rightarrow$	Neutral	
1	9	7	2	2	2
2	7	2	2	0	0
3	2	2	1	0	0
4	2	0	0	0	0
5	2	0	0	0	0

Table 9. Percentage of normalized deviation of inductance from that of reference: Case-D

From the synthesized circuit, it is seen that the capacitance matrix has remained unchanged (signifying fault is not capacitive), whereas, inductance matrix shows many changes. For easier interpretation, the normalized difference matrix (i.e. ratio of the difference between $[L_{est,D}]$ and $[L_{ref}]$ to L_{max}, where L_{max} is the diagonal element of $[L_{ref}]$) is calculated and shown in Table 9. From this it is observed that, maximum change in inductance has occurred at element L_{11}, which refers to Section 1 or line-end. So, the inductive change has been correctly identified, as well as, localized. As mentioned earlier, when there is a short-circuit (i.e. inductance changes), there is observed a widespread change to elements in $[L]$. This is evident in the difference matrix. But, the row and column index corresponding to maximum change (shown as shaded) points to the location of the change. Thus, localization and type of change have been accurately identified.

7.3 Case-E, Inductive Change in the Middle

This is an example wherein the type-of-change is same as in Case-D, but its position has been moved from the line-end (disc 2 and 3) to the middle (disc 8 and 9). All other aspects are the same. The overall change in effective inductance was 220 μH. Results for this case were obtained. Table 10 summarizes the measured and estimated ocnf and scnf.

ocnf (kHz)	Measured	216	399
	Estimated	219.1	407.6
scnf (kHz)	Measured	336	-
	Estimated	340.8	-

Table 10. Measured and estimated natural frequencies for an actual transformer winding (interleaved) - Case E

The match between them is evident. As anticipated, the capacitance matrix has remained unchanged while the inductance matrix shows changes. The normalized difference between

$[L_{ref}]$ and $[L_{est,E}]$ is calculated and is shown in Table 11. Compared to the results of the previous case, the maximum change has now shifted to exactly the middle of the winding, i.e. node 3. Thus, localization and type of change have been accurately identified.

Node	Line		⇒	Neutral	
1	1	2	0	0	0
2	2	2	2	0	0
3	0	2	16	14	3
4	0	0	14	9	7
5	0	0	3	7	1

Table 11. Percentage of normalized deviation of inductance from that of reference: Case-E

7.4 Case-F, Capacitive and Inductive Changes at Physically Different Locations

This case pertains to simultaneous inductive and capacitive changes, occurring at different locations. This was achieved by imposing a short-circuit between the outermost turns of disc 14 and 15, and by addition of a lumped capacitance of 50 pF between outermost turn of disc 6 and ground. With this condition imposed, swept frequency measurements were completed. The

ocnf	Measured	204	402	541
(kHz)	Estimated	200.6	403.8	537.3
scnf	Measured	354	508	-
(kHz)	Estimated	348.8	500.6	-

Table 12. Measured and estimated natural frequencies for an actual transformer winding (interleaved) - Case F

effective inductance showed a change of 200 μH, while effective shunt capacitance changed by 50 pF. Using the proposed approach, the following results were obtained. Table 12 is a comparison of measured and estimated natural frequencies pertaining to this case and from which it is evident that the agreement is reasonably good. The capacitance and inductance matrices of the synthesized circuit are given below from which location and extent of change can be easily determined.

Cg_1	Cg_2	Cg_3	Cg_4	Cg_5
0.019	0.059	0.029	0.129	0.184

Table 13. Estimated shunt capacitance (in nF) for an actual transformer winding (interleaved): Case-F

$$L_{est,F} = \begin{bmatrix} 0.440 & 0.215 & 0.090 & 0.080 & 0.065 \\ 0.215 & 0.435 & 0.215 & 0.085 & 0.070 \\ 0.090 & 0.215 & 0.435 & 0.210 & 0.080 \\ 0.080 & 0.085 & 0.210 & 0.390 & 0.165 \\ 0.065 & 0.070 & 0.080 & 0.165 & 0.350 \end{bmatrix} \quad (3)$$

Node	Line		⇒	Neutral	
1	0	1	0	1	3
2	1	1	1	1	3
3	0	1	1	2	2
4	1	1	2	11	13
5	3	3	2	13	20

Table 14. Percentage of normalized deviation of inductance from that of reference: Case-F

From the normalized difference matrix presented in Table 14, it is seen that the last row and column has undergone the maximum change, signifying that the self-inductance in the last section (i.e. neutral-end) has changed. The estimated capacitance matrix (in Table 13) shows that shunt capacitance at node 2 and node 3 has increased by 40 pF and 10 pF respectively. Such a change is understandable, since disc number 6 maps to node 2 in the synthesized circuit. So, the overall estimation seems reasonably accurate, both in terms of localization, as well as, in discriminating the type of change. Also, two changes occurring at physically different locations could be localized.

7.5 Mapping of Winding Discs to Sections in Synthesized Circuit

Localization of inductive and/or capacitive changes introduced at various positions along a transformer winding was successfully demonstrated. The localization accuracy was uniformly good for all cases. As a consequence of these case studies, a mapping between winding discs and the sections of the synthesized circuit can be visualized, and this is shown in Fig. 13. From this, it is evident that approximately every three winding discs are mapped to one section in the synthesized circuit. Further, it is obvious that shorting of discs 6 and 7, 10 and 11, etc. would not map onto a single discrete node in the synthesized circuit. Hence, under such fault condition it is natural that the synthesized circuit would show some changes at the adjacent sections also.

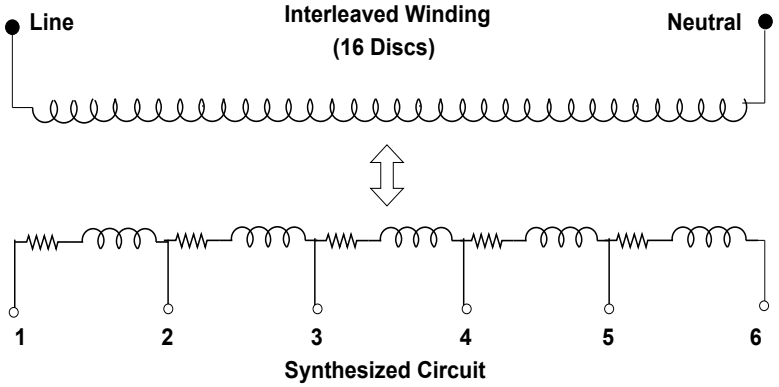

Fig. 13. Mapping of discs in actual winding to sections in synthesized circuit (series and shunt capacitances exist in synthesized circuit, but, those are not shown)

7.6 Scope for Improvement

The proposed method, involving circuit synthesis using measured data, required the selection of some parameters. In the absence of any other reliable method of predetermining them, an iterative solution was pursued. The upper and lower limits of each parameter and their increments were progressively fine-tuned by a trial and error method. Obviously, a compromise had to be made between time required for convergence and the degree of match achievable between measured and estimated characteristics. With a tolerance limit set to 2%, a reasonably good agreement was achievable. The method involved an iterative brute-force search strategy and was very time-consuming. As a matter of fact, the time taken to synthesize even a small 5-section ladder network was of the order of a few tens of hours. This aspect was indeed a shortcoming that prevented its further usage. To make this approach practically attractive, some means of reducing this processing time had to be explored. This matter is explained in the next section.

8. Time-Efficient Algorithm for Synthesizing Large-Sized Ladder Networks

A fully interleaved winding contains very few observable and measurable natural frequencies, typically 2 or 3. So, the circuit to be synthesized was small and could be handled by the iterative procedure. Whereas, in contrast, a disc winding contains a large number of regularly spaced natural frequencies, typically 8 to 10. The corresponding ladder network to be synthesized in this case is likely to have about 10 to 12 sections, i.e., a large-sized network. Hence, the FRA data pertaining to a disc winding was utilized here.

The objective of synthesizing a suitable ladder network corresponding to the measured terminal characteristics of a transformer winding can be construed as a constrained optimization problem. Through optimization techniques it is possible to overcome the shortcoming of the earlier described brute-force iterative search approach. The proposed solution approach, explained below, essentially involves formulating an objective function and minimizing it.

1. Formulation of the objective function
   As the goal is to synthesize a circuit having the same set of natural frequencies as that of the transformer winding, the objective function can be considered as the difference between the measured natural frequencies of the transformer winding ($f_{measured}$) and the estimated natural frequencies of the synthesized circuit ($f_{estimated}$). Hence, the objective function can be written as,

   $$g = f_{estimated} - f_{measured} \tag{4}$$

   where,
   $f_{measured}$ - natural frequencies identified from measured FRA plot
   $f_{estimated}$ - natural frequencies estimated using synthesized circuit

2. Enforcing constraints
   As the problem is open-ended, obviously it will have multiple solutions. In order to limit the number of feasible solutions, the following constraints need to be enforced. Hence, the objective can be restated as, minimizing the objective function g, subject to the following constraints.

   - As the effective value of the shunt capacitance of the synthesized circuit should match with that of the measured value on the transformer winding, one of the equality constraints can be formulated as,

$$C_{g,eff}(estimated) = C_{g,eff}(measured) \tag{5}$$

- For the chosen configuration of the winding (as in Fig. 2), shunt capacitances can be chosen to be equal in magnitude up to 50% of the physical length of the winding, beyond which, it can be considered to monotonically increase in magnitude due to the closer vicinity of the ground plane to the discs closer to the neutral. This equality and inequality constraints on the disposition of shunt capacitances are mentioned below.

$$\begin{array}{ll} C_g(1) = C_g(2) = \cdots = C_g(\frac{N}{2}) & \\ C_g(k) < C_g(k+1), & k = \frac{N}{2}, \cdots, N-1 \end{array} \tag{6}$$

- Equality constraint on the effective value of the inductance of the winding is -

$$L_{eq}(estimated) = L_{eq}(measured) \tag{7}$$

- The mutual inductance between a given disc and other discs decreases as their separation distance increases. This fact can effectively be captured by describing an inequality constraint (connecting mutual inductances) as given below.

$$\begin{array}{ll} m_1 < l_s & \\ m_k < m_{k-1}, & k = 2, \cdots, N-1 \end{array} \tag{8}$$

The algorithm described above was coded and initially tested with FRA data presented in Section 7, on a fully interleaved winding. The reference circuit was obtained within a matter of few seconds and the estimated and measured characteristics matched very well. In order to test the capability of this alternative approach to synthesize large-sized ladder networks, the FRA data pertaining to a disc winding (with 16 discs) was considered next. It contained about 8-9 natural frequencies from which a 9-10 section ladder network could be anticipated to be synthesized. The important steps in realization of the circuit are explained in the following sections.

8.1 Circuit Synthesis for Disc Winding - Reference Case

The terminal characteristics of a disc winding pertaining to the un-faulted (or healthy) case is considered and the corresponding synthesized circuit is referred to as the reference circuit.

- Parameters pertaining to the disc winding are measured and mentioned below.
  R = 0.3 Ω, L_{eq} = 2.03 mH, $C_{g,eff}$ = 0.22 nF.
- With the neutral of the winding grounded, FRA is performed on the disc winding and is shown in Fig. 14(a). From the acquired FRA data, open-circuit and short-circuit natural frequencies are identified and tabulated in Table 15.

(NOTE: The measured natural frequencies of the disc winding show frequencies up to about 5.5 MHz. In practice one observes these natural frequencies well within 1.0 to 1.5 MHz. Since the transformer winding was small in size, it was natural to expect the natural frequencies to be scaled up by the same factor. Intentionally, no scaling was employed to the measured winding parameters. Therefore, using this raw measured data the resulting synthesized circuit had low values of capacitances and inductances. This was naturally anticipated. As the main aim of this section was to examine the

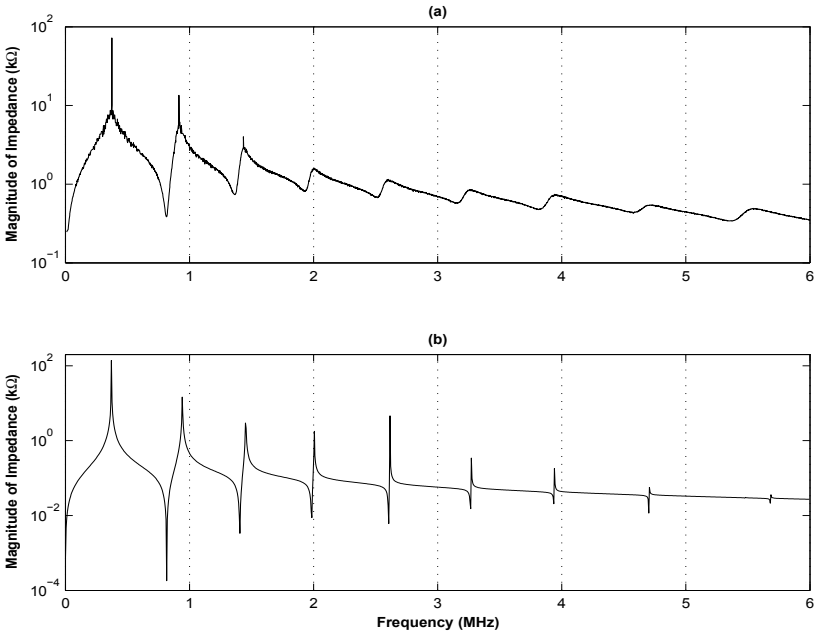

Fig. 14. Driving-point impedance for an actual disc winding, Reference Case, (a) Measured, (b) Estimated from synthesized circuit shown in Fig. 15

ocnf	Measured	370	927	1463	2033	2650	3314	4008	4765	5618
(kHz)	Estimated	371	942	1453	2005	2616	3270	3942	4703	5480
scnf	Measured	832	1391	1963	2552	3198	3872	4655	5332	-
(kHz)	Estimated	816	1405	1984	2605	3265	3939	4702	5480	-

Table 15. Measured and estimated natural frequencies for a disc winding - Reference case

capability to convert an FRA data into a synthesized circuit, no scaling of data was undertaken prior to using them.)

Since the FRA exhibits 9 open-circuit natural frequencies, number of sections in the circuit to be developed should be greater than or equal to 9. The proposed algorithm converges to the circuit described in Fig. 15. Values of mutual inductances between any two inductors of the synthesized circuit are given in Table 16. The circuit so synthesized has the natural frequencies (Fig. 14(b)) which are within 3% of tolerance level of those identified from FRA in Fig. 14(a).

L_s	$M_{i,i+1}$	$M_{i,i+2}$	$M_{i,i+3}$	$M_{i,i+4}$	$M_{i,i+5}$	$M_{i,i+6}$	$M_{i,i+7}$	$M_{i,i+8}$	$M_{i,i+9}$
0.0434	0.0325	0.0214	0.0142	0.0100	0.0067	0.0053	0.0037	0.0030	0.0023

Table 16. Self and mutual inductances (in mH) for circuit in Fig. 15

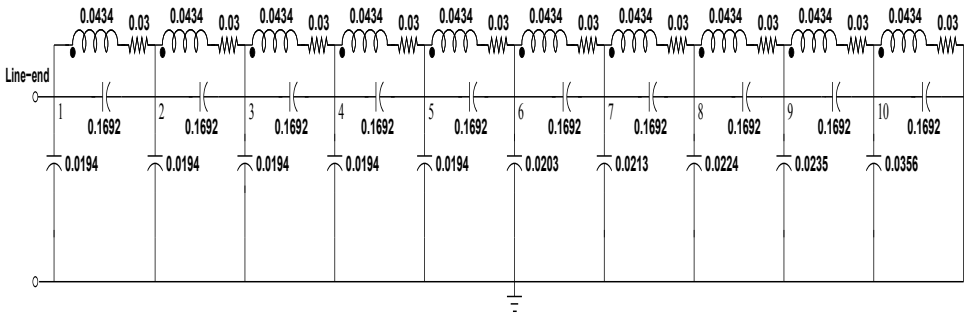

Fig. 15. Synthesized reference circuit pertaining to disc winding (Note: Elemental values are in Ω, nF, mH. Mutual inductances of synthesized circuit are given in Table 16)

8.2 Circuit Synthesis for Disc Winding After Changes - Fault Case

To simulate a fault case, an additional capacitance of 30 pF was added between the start of disc 8 and ground. How this change gets reflected in the synthesized circuit is explained below.

- Parameters pertaining to the changed system are determined.
  R = 0.3 Ω, L_{eq} = 2.03 mH, $C_{g,eff}$ = 0.249 nF.
- For the changed system, FRA is performed and shown in Fig. 16(a). From the FRA data, the natural frequencies are identified and tabulated in Table 17.

ocnf	Measured	351	870	1448	1981	2608	3245	3960	4691	5546
(kHz)	Estimated	355	909	1453	1981	2616	3249	3942	4695	5452
scnf	Measured	743	1368	1911	2512	3124	3820	4572	5351	-
(kHz)	Estimated	756	1405	1963	2605	3241	3939	4694	5452	-

Table 17. Measured and estimated natural frequencies for a disc winding - Fault case

The algorithm converges to the synthesized circuit shown in Fig. 17 within 10-20 seconds. However, a few of the frequencies of the synthesized circuit (Fig. 16(b)) differ from those measured by 3-5%. To start with, this result can be taken as acceptable. This difference can be reduced further by fine-tuning the algorithm. However, it was not undertaken at the present moment. Perhaps, it may also be due to the fact that a winding with 16-discs is mapped on to a circuit with 10-sections. The accuracy achieved with the proposed optimization is reasonable. Further, it is worth mentioning that the algorithm converges within a very short time (in the order of a few tens of seconds). Hence, it is possible to address the following needs viz. finer representation of the winding, circuit realization of multi-winding transformer, etc. This was not achievable by the earlier approaches in spite of powerful computing machines. Research in this direction would continue and aid in localization of winding deformations and/or faults and in quantifying them in an actual multiwinding transformer.

9. Scope of Future Work

Some thoughts for future work revolve around the localization problem on multiple winding transformers and can be tackled as follows-

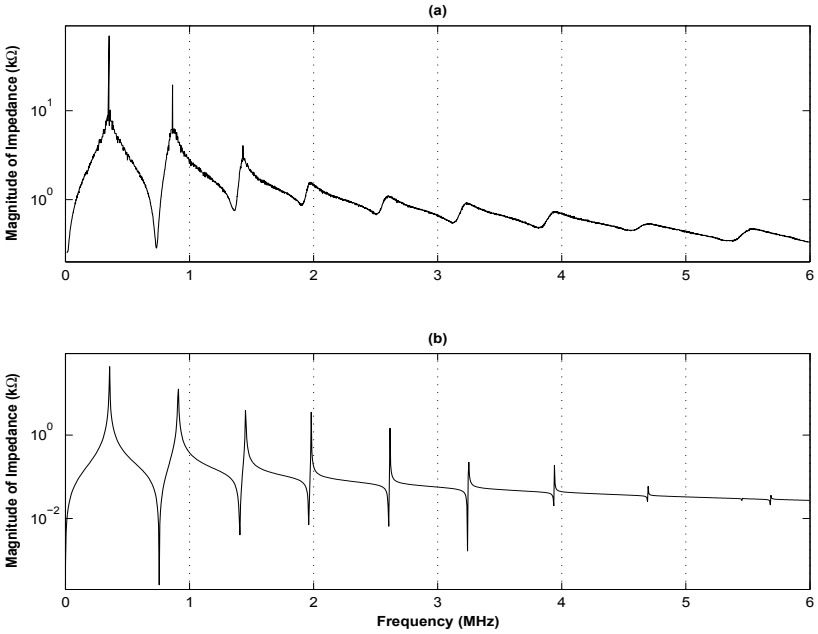

Fig. 16. Driving-point impedance for an actual disc winding, Fault Case, (a) Measured, (b) Estimated from synthesized circuit shown in Fig. 17

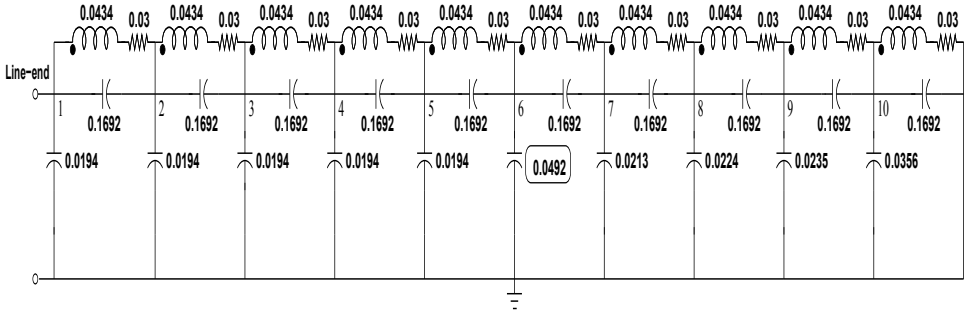

Fig. 17. Synthesized circuit pertaining to disc winding after changes (Note: Elemental values are in Ω, nF, mH. Mutual inductances of synthesized circuit are in Table 16)

1. A separate ladder network is required to represent each winding of a transformer and each of these networks must be linked to the immediate neighbour by the inter-winding capacitances.
2. To synthesize a ladder network corresponding to a winding, FRA must be conducted on that particular winding, keeping all the rest of the windings short-circuited and

connected to ground. Imposing this terminal condition ensures minimum influence of neighbouring windings on the tested winding during measurement.

3. A comparison of the subsequently synthesized ladder networks with the reference case can assist in localization of deformation.
4. A sacrificial transformer unit must be identified for this purpose, so that actual deformations (like radial, axial, etc.) can be incorporated to examine the true potential of the proposed method.

Future research efforts will pursue these ideas.

10. Conclusions

This chapter presents a mathematical approach to tackle the problem of localization of deformations in transformer windings. The approach essentially comprises of converting the measured driving-point impedance (via circuit synthesis) into a physically realizable, mutually coupled, ladder network that reproduces the measured characteristics as closely as possible. From a comparison of such synthesized circuits with the reference circuit, it is possible to assess the extent of damage the winding has undergone, in terms of the observed changes in the values of pertinent circuit elements.
The task of localizing discrete changes was demonstrated using a model winding and an actual transformer winding. The localization accuracy achieved was reasonably good in all the experimental cases presented. Nevertheless, it is impossible to use this iterative technique to address the localization problem in practice. This is mainly because, the process is extremely slow when large-sized circuits have to be synthesized, as it employs a brute-force search strategy. This shortcoming was recognized and a far more superior and time-efficient alternative was suggested. One such idea, based on constrained-optimization technique was presented and discussed at the end of this chapter. The algorithm is still in the developmental stages and hence only preliminary results are reported. In spite of it, from the results presented it is clear that this method is highly time-efficient. It required only a few tens of seconds to synthesize a mutually coupled, 10-section ladder network. Therefore, it seems to be well suited to synthesize many such large-sized circuits rapidly, corresponding to each winding in a transformer. This feature makes it an ideal candidate for addressing the ultimate problem of localization of winding deformation in multi-winding transformers. In final summary, it is believed that with the suggested method, we are better equipped to address the problem of deformation localization in an actual multi-winding transformer.

11. Acknowledgements

We thank research students, Mr. Saurav Pramanik and Mr. Santosh C Vora, of High Voltage Laboratory, Department of Electrical Engineering, Indian Institute of Science, India, for their assistance in conducting experiments and acquiring frequency response data pertaining to an actual disc winding used in this work.

12. References

[1] Dick, E. P. & Erven, C. C. (1978). Transformer Diagnostic Testing by Frequency Response Analysis. *IEEE Trans. Power Apparatus and Systems*, vol. PAS-97, Nov./Dec. 1978, pp. 2144-2153.

[2] Florkowski, M. & Furgal, J. (2003). Detection of Transformer Winding Deformations Based on the Transfer Function Measurements and Simulations. *Journal Meas. Sci. Tech.*, 14, 2003, pp. 1986-1992.
[3] Gustavsen, Bjorn & Semlyen, Adam (1999). Rational Approximation of Frequency Domain Responses by Vector Fitting. *IEEE Trans. Power Delivery*, vol. 14, no. 3, Jul. 1999, pp. 1052-1061.
[4] Islam, S. M. (2000). Detection of Shorted Turns and Winding Movements in Large Power Transformers using Frequency Response Analysis. *IEEE Power Engineering Society Winter Meeting. Conference Proceedings*, vol.3, pt. 3, 2000, pp. 2233-2238.
[5] Lech, W. & Tyminski, L. (1966). Detecting transformer winding damage- the low voltage impulse method. *Electrical Review*, no. 18, 1966.
[6] Morched, A.; Martf, L. & Ottevangers, J. (1993). A High Frequency Transformer Model for the EMTP. *IEEE Trans. Power Delivery*, vol. 8, no. 3, Jul. 1993, pp.1615-1626.
[7] Oguz Soysal, A. (1993). A Method for Wide Frequency Range Modeling of Power Transformers and Rotating Machines. *IEEE Trans. Power Delivery*, vol. 8, no. 4, Oct. 1993, pp. 1802-1808.
[8] Ragavan, K. & Satish, L. (2007). Localization of Changes in a Model Winding based on Terminal Measurements: Experimental Study. *IEEE Trans. Power Delivery*, vol. 22, no. 3, July 2007, pp. 1557-1565.
[9] Rahimpour, E.; Christian, J.; Feser, K. & Moheseni, H. (2003). Transfer Function Method to Diagnose Axial Displacement and Radial Deformation of Transformer Windings. *IEEE Trans. Power Delivery*, vol. 18, Apr. 2003, pp. 493-505.
[10] Ryder, S. A. (2003). Diagnosing transformer faults using frequency response analysis. *IEEE EI Magazine*, vol. 19, no. 2, Mar.-Apr. 2003, pp.16-22.
[11] Satish, L. & Subrat K. Sahoo (2009). Locating Faults in a Transformer Winding: An Experimental Study. *Electric Power Systems Research*, vol. 79, 2009, pp. 89-97.
[12] Satish, L. & Santosh C. Vora (2009). Amplitude Frequency Response Measurement - A Simple Technique. *IEEE Trans. Education*, 2009, in press.

Fault Detection

Edited by Wei Zhang

ISBN 978-953-307-037-7
Hard cover, 504 pages
Publisher InTech
Published online 01, March, 2010
Published in print edition March, 2010

In this book, a number of innovative fault diagnosis algorithms in recently years are introduced. These methods can detect failures of various types of system effectively, and with a relatively high significance.

How to reference

In order to correctly reference this scholarly work, feel free to copy and paste the following:

Satish L and Ragavan K (2010). Recent Advances in Localization of Winding Deformation in a Transformer, Fault Detection, Wei Zhang (Ed.), ISBN: 978-953-307-037-7, InTech, Available from: http://www.intechopen.com/books/fault-detection/recent-advances-in-localization-of-winding-deformation-in-a-transformer

INTECH
open science | open minds

InTech Europe
University Campus STeP Ri
Slavka Krautzeka 83/A
51000 Rijeka, Croatia
Phone: +385 (51) 770 447
Fax: +385 (51) 686 166
www.intechopen.com

InTech China
Unit 405, Office Block, Hotel Equatorial Shanghai
No.65, Yan An Road (West), Shanghai, 200040, China
中国上海市延安西路65号上海国际贵都大饭店办公楼405单元
Phone: +86-21-62489820
Fax: +86-21-62489821